ISSN 1061-933X, Colloid Journal, 2017, Vol. 79, No. 1, pp. 94–105. © Pleiades Publishing, Ltd., 2017.
Original Russian Text © E.A. Podorozhko, G.R. Ul'yabaeva, V.E. Tikhonov, A.V. Grachev, L.V. Vladimirov, Yu.A. Antonov, N.R. Kil'deeva, V.I. Lozinsky, 2016, published in Kolloidnyi Zhurnal, 2016, Vol. 78, No. 6, pp. 760–771.

A Study of Cryostructuring of Polymer Systems. 43. Characteristics of Microstructure of Chitosan-Containing Complex and Composite Poly(vinyl alcohol) Cryogels

E. A. Podorozhko[a], G. R. Ul'yabaeva[b], V. E. Tikhonov[a], A. V. Grachev[c], L. V. Vladimirov[c], Yu. A. Antonov[d], N. R. Kil'deeva[b], and V. I. Lozinsky[a]*

[a] *Nesmeyanov Institute of Organoelement Compounds, Russian Academy of Sciences, ul. Vavilova 28, Moscow, 119991 Russia*
[b] *Moscow State University of Design and Technology, ul. Sadovnicheskaya 33/1, Moscow, 117997 Russia*
[c] *Semenov Institute of Chemical Physics, Russian Academy of Sciences, ul. Kosygina 4, Moscow, 119991 Russia*
[d] *Emanuel Institute of Biochemical Physics, Russian Academy of Sciences, ul. Kosygina 4, Moscow, 119334 Russia*
**e-mail: loz@ineos.ac.ru*

Received May 31, 2016

Abstract—The microstructure of complex and composite poly(vinyl alcohol) (PVA) cryogels containing water-soluble chitosan hydrochloride (ChHC) of dispersed particles of water-insoluble chitosan base (Ch), respectively, has been studied by optical microscopy and attenuated total reflection FTIR spectroscopy. The macroporous morphology of cryogels has been studied using preparations in the form of thin (~10 μm) sections and discs 1 mm thick. The introduction of non-gelling additives (NaCl and ChHC) into an initial PVA solution causes significant changes in the size and shapes of macropores in the complex cryogels formed by freezing–defrosting, as compared with the pores in the samples obtained under the same conditions without additives. The reasons for the changes are the process of phase segregation and the influence of low- and high-molecular-weight electrolytes on crystallization of ice, which plays the role of a porogen upon cryotropic gelation of aqueous PVA solutions. As a result of an alkaline treatment of the complex cryogels, which transforms ChHC into Ch, microcoagulation of chitosan yields discrete, almost spherical, particles with sizes of about 1–5 μm. IR spectral studies have shown that concentration gradients of the gelling and nongelling polymers arise along the thickness of the gel discs, with PVA concentration prevailing near the lower surface and ChHC or Ch concentration dominating near the upper surface of the disc.

DOI: 10.1134/S1061933X16060119

INTRODUCTION

Poly(vinyl alcohol) cryogels **(**PVACGs) are crystallization-type macroporous gels that result from freezing concentrated solutions of the polymer, followed by their incubation in the frozen state and subsequent defrosting [1–7]. As a rule, water or dimethyl sulfoxide is used as a dispersion medium. If an initial poly(vinyl alcohol) (**PVA**) solution contains additives of some other low- and/or high-molecular-weight compounds, *complex* PVACGs are formed after the cryogenic treatment. When a discrete phase (solid particles, microdroplets of an immiscible liquid, or small gas bubbles) is present in an initial mixture, the freezing–defrosting of such dispersions results in the formation of *filled* (*composite*) PVA cryogels. All these three types of PVACGs are increasingly applied in various practical fields ranging from medicine [1–4, 8–15] and biotechnology [3, 16–24] to building engineering [3, 25–27] and ecology [28], thereby determining the urgency of detailed studying these gel systems.

Our previous study [29] in this field dealt with the preparation and investigation of the physical-mechanical and thermophysical properties of complex PVACGs formed in the presence of a water-soluble polymer, chitosan hydrochloride (ChHC), and in the absence or presence of a low-molecular-weight electrolyte (0.15 M NaCl). An alkaline treatment of these complex PVACGs transformed chitosan hydrochloride into the water insoluble form, chitosan base (Ch), the dispersed particles of which appeared to be included into the continuous gel phase as a filler; i.e., complex cryogels were transformed into composite PVACGs. Rigidity, heat endurance, and the sorption characteristics of the filled cryogels with respect to copper(II) ions were determined. All these studies showed that the microstructure of the aforementioned gel preparations has a substantial effect on the integral characteristics of both complex and composite PVACGs. This made it necessary to additionally study the structure and pore morphology of the PVACGs. Such study has become the goal of this work per-

formed with the help of optical microscopy and IR spectroscopy. The obtained experimental results are considered in this communication.

EXPERIMENTAL

As in [29], the following compounds and preparations were used as received: poly(vinyl alcohol) with molecular mass MM = 86 kDa and degree of deacetylation of 100% (Acros Organics, United States), sodium chloride (>99%) (Aldrich, United States), and an aqueous 25% ammonia solution (Reakhim, Russia). Chitosan hydrochloride with a molecular mass of 45.6 kDa and the degree of deacetylation equal to 97% was obtained by controlled acidic hydrolysis of high-molecular-mass chitosan according to the procedure described in [30].

Experimental details of the preparation of initial water–PVA–ChHC and water–PVA–ChHC–NaCl solutions, regimes of the formation of complex cryogels from them, and the subsequent transformation of ChHC into water-insoluble Ch, which was, in the long run, incorporated into PVA cryogel continuous phase as a dispersed filler, by alkaline treatment had been described in [29]. All cryotropic gelation processes were carried out under the same conditions, namely, freezing of initial solutions at –20°C for 12 h was followed by defrosting of the samples at a rate of 0.03°C/min, which was preset by the microprocessor of an FP 45 HP programmed cryostat (Julabo, Germany).

The morphology of the cryogels was studied using an Eclipse 55i optical microscope (Nikon, Japan) equipped with a digital system for image registration. For the experiments, which were performed by the previously described procedure [31, 32], thin (~10 μm) sections were cut in the directions perpendicular and parallel to the axes of cylindrical samples formed in dismountable duralumin containers with an internal diameter and a height of 15 and 10 mm, respectively. The sections were stained in an aqueous Congo red solution. Before the examinations, the preparations were stored at 4°C in sealed containers.

In addition, cryogel samples were prepared as discs 1 mm thick in plastic Petri dishes (internal diameter of 36 mm). After the molding, the PVACG discs were washed with water for 24 h to remove a soluble sol fraction, stained in an aqueous 1% Congo red solution for 1 min, and then washed with water to remove excess dye.

The porous morphology of the two surfaces of the resulting gel discs was studied by optical microscopy.

—The lower surface had been in contact with the bottom of the Petri dish during PVACG molding.

—The upper surface had been in contact with air in the course of PVACG molding.

IR spectroscopic examinations of the lower and upper surfaces of analogous PVACG preparations were carried out using a Vertex 70 FTIR spectrometer (Bruker, United States). The spectra were recorded at a resolution of 2 or 4 cm^{-1} by the method of attenuated total reflection (ATR) using a GladiATR attachment (Pike Technologies, United States) and a diamond internal reflection element (number of reflections n = 2 and 4 and radiation incidence angle of 45°). The spectra were recorded and processed using the Bruker Opus software package (Version 7.0).

RESULTS AND DISCUSSION

Study of the Microstructure of Thin Sections of Complex and Composite PVA Cryogels Containing Inclusions of ChHC and Ch, Respectively

Earlier, the study of the properties of chitosan-containing complex and composite PVACGs showed that their physical-mechanical and thermophysical properties were mainly governed by ChHC concentration in an initial solution and the presence or absence of a low-molecular-weight salt (NaCl) in it, as well as the concentration of filler particles formed in a composite cryogel after the transformation of ChHC into Ch [29]. As regards the influence of the aforementioned or other possible factors on the microstructure of such complex and composite heterophase gels, the problem needed a more detailed study, the results of which are discussed below.

In particular, Fig. 1 exemplifies micrographs of thin sections of PVACGs (polymer concentration of 120 g/L) obtained in the absence of ChHC without and with salt additives (0.15 mol/L NaCl) (Figs. 1a and 1b, respectively), as well as ChHC-containing (56 g/L) complex cryogels also prepared without and with NaCl (Figs. 1c and 1d, respectively). The preparations for these microscopic studies were prepared by cutting them with a microtome from the middle parts of cylindrical samples of cryogels with a height of 10 mm and a diameter of 15 mm. In the black-and-white images, the dark regions show the polymer phase, i.e., the gel walls of macropores stained with Congo red (see Experimental), while the light areas depict the water-filled macropores in the heterophase material.

It is known [33] that the addition of NaCl to PVA solutions used for the preparation of PVACGs causes modification of the microtexture and, accordingly, the porosity parameters of the resulting cryogels. At the qualitative level, a similar effect was also observed in this study; i.e., the morphology of the water–NaCl–PVA preparation (Fig. 1b) somewhat changed relative to that of the salt-free sample (Fig. 1a). The cross-sectional sizes of macropores decreased from 4–5 to 1–3 μm, and the texture became more diffuse. The reasons for these changes were the influence of the salt on ice formation (the geometry and sizes of its crystals [34, 35], which play the role of a porogen upon cryotropic gelation [3, 6, 7, 31, 36–38]) and, seemingly, the salting-out effect of NaCl on PVA in the

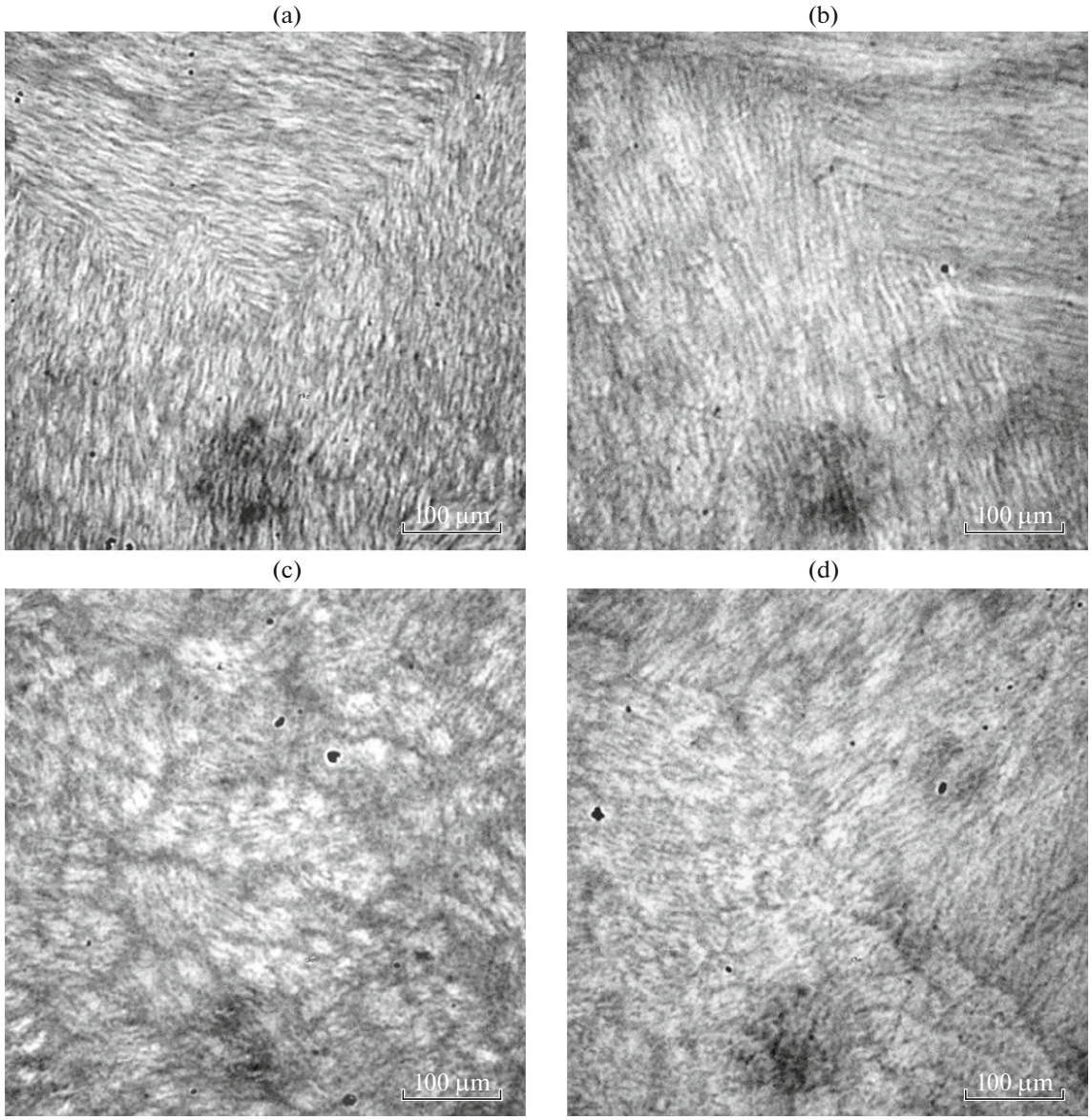

Fig. 1. Micrographs of PVACGs thin sections perpendicular to the axes of cylindrical samples: (a) a cryogel formed from an aqueous PVA solution (120 g/L), (b) a cryogel formed from an aqueous PVA solution (120 g/L) in the presence of NaCl (0.15 mol/L), (c) a complex cryogel formed from a mixed aqueous solution of PVA (120 g/L) and ChHC (56 g/L), and (d) a complex cryogel formed from a mixed aqueous solution of PVA (120 g/L) and ChHC (56 g/L) in the presence of NaCl (0.15 mol/L).

bulk of the so-called "unfrozen liquid microphase" (ULMP) [39], in which both these components of the macroscopically frozen system were concentrated. In turn, the microstructure of complex PVACGs obtained by freezing–defrosting of water–PVA–ChHC or water–NaCl–PVA–ChHC mixed solutions differed from that of corresponding samples free of the additives of the polymer electrolyte (ChHC). In particular, macropores of the water–PVA–ChHC cryogel acquired a roundish shape (compare Figs. 1a and 1b), while distinct regions with an increased PVA density (dark strands in Fig. 1d) were observed in the structure of the water–NaCl–PVA–ChHC cryogel. These changes in the macroporous morphology of these complex cryogels resulted from the simultaneous participation of a number of processes in the formation of their structure. For example, polymer electrolyte additives (ChHC is not a gelling polymer [29]) increase the ionic strength of the system, i.e., promote the salting out of the gelling polymer, which may be one reason for the formation of the regions with an increased density of the PVA-containing phase (Fig. 1d). Even the very presence of different ions in the system being frozen influences, as has been noted above, the shape and size of ice crystals, thereby affecting the geometry of macropores in a

cryogel resulting from defrosting. Finally, water crystallization upon freezing of mixed solutions of PVA and ChHC, which causes them to concentrate in ULMP, leads (especially in the presence of NaCl [29]) to solution separation into two liquid phases. One of the phases is enriched with PVA and the gelation is, actually, realized in it. The other phase is enriched with ChHC, the solution of which fills cryogel pores upon the defrosting of the samples and, then, is washed out of them during the preparation of thin sections for microscopic examinations.

It is known [40–42] that the effects of concentration-induced liquid phase separation may significantly modify the texture of PVACGs up to the formation of very large pores in them, with the modification being, of course, determined by the chemical nature, molecular-mass characteristics, and initial concentrations of gelling and nongelling polymers in a common solvent. We think that large pores with cross-sectional sizes of 10–50 μm observed in the micrographs (Figs. 1c, 1d) are "replicas" of the phase enriched with nongelling ChHC, which is, then, washed out with water from the thin sections of the preparations (see Experimental). It should also be noted that, as in the case of ChHC-free PVACGs (Figs. 1a, 1b), the presence of the low-molecular-weight salt in the complex water–NaCl–PVA–ChHC cryogel leads to a decrease in the cross-sectional sizes of macropores and a more diffused morphology of the samples (Fig. 1d) as compared with the complex water–PVA–ChHC cryogel (Fig. 1c).

Subsequent treatment of the ChHC-containing PVACGs with alkaline agents (first, in ammonia atmosphere and, then, in an aqueous NaOH solution [29]) transformed ChHC into the water-insoluble base form. This resulted in the transformation of the complex cryogels into composite ones, the continuous macroporous gel phase of which contained small particles of Ch coagulate dispersed as a filler. Micrographs of the thin sections of such composite cryogels formed from initial solutions of PVA and ChHC containing 56 and 112 g/L of the nongelling polymer are shown as an example in Fig. 2. In the micrographs, the Ch phase appears as discrete, dark, almost spherical particles with sizes of about 1–5 μm.

Attention is drawn by the difference between the micrographs of the transverse (Figs. 2a, 2b) and longitudinal (Figs. 2c, 2d) sections. In the first case, Ch particles are almost uniformly distributed over the micrograph, although regions with somewhat different filler densities can be seen. Micrographs in Figs. 2a and 2b differ in the number of the particles: at the higher initial concentration of chitosan salt, more Ch microspheres are, expectedly, included into the continuous phase of the cryogel. On the contrary, regions with different densities of the dispersed filler oriented in the same direction are distinctly seen in the longitudinal sections of the composite PVACGs (especially in Fig. 2c). Since such thin sections were prepared from cylindrical PVACG samples formed by freezing of the initial solutions located in metal containers, which were placed onto a cooling horizontal plate in a cryostat chamber to freeze the samples, a gradient of heat removal from the preparations was directed along the cylinder axis. Therefore, the front of ice crystallization moved predominantly in this direction. As a consequence, the cryoconcentration of PVA and ChHC in the bulk of ULMP, as well as the aforementioned separation of the liquid phase in the intercrystalline space were "oriented" along the cylinder axis. Then, the cryotropic gelation, which took place in the system, transformed the PVA-enriched liquid phase into a gel, and subsequent alkaline treatment of complex PVACGs with the purpose to transform of ChHC into Ch fixed the orientation of the phases segregated predominantly in the direction of the growth of ice crystals. This seems to be the reason for the fact that the nonuniform density distribution of filler particles is better seen in the longitudinal sections (Figs. 2c, 2d) than in the transverse sections (Figs. 2a, 2b) of the composite cryogels.

The micrographs presented in Figs. 1 and 2 show the macroporous morphology of cryogel samples prepared as thin (~10 μm) sections using a freezing microtome [31, 32]. In this case, the gel material had been subjected to some additional physical actions during freezing and cutting. In this context, a procedure potentially more "sparing" with respect to the microstructure of the samples is the formation of PVACGs as plates or disks so thin that they could be used for examinations by transmission optical microscopy [29, 42, 43]. Preliminary experiments have shown that, for the complex PVACGs studied in this work, the thickness of the samples should be no more than 1 mm. However, the samples of composite PVACGs with the same thickness appeared, unfortunately, to be too turbid; therefore, we confined ourselves to the investigation of only thin sections shown in Fig. 2 for them.

Characteristics of Macroporous Morphology of PVACGs Formed as Discs 1 mm Thick

The micrographs depicted in Figs. 3 and 4 show variations in the morphology of the lower and the upper surfaces of cryogel samples prepared as discs 1 mm thick from water–PVA–ChHC (Fig. 3) and water–NaCl–PVA–ChHC (Fig. 4) solutions with concentrations of nongelling polymer ChHC in an initial 120 g/L PVA solution increasing from 56 to 112 and 156 g/L. When such solutions are frozen in plastic Petri dishes placed on a cooled plate, a decreasing temperature gradient is directed upward; therefore, the ice crystals' growth occurs in the same direction, which, in principle, must lead to a certain vertical orientation of macropores in a cryogel being formed. In particular, this effect took place when cryostructuring

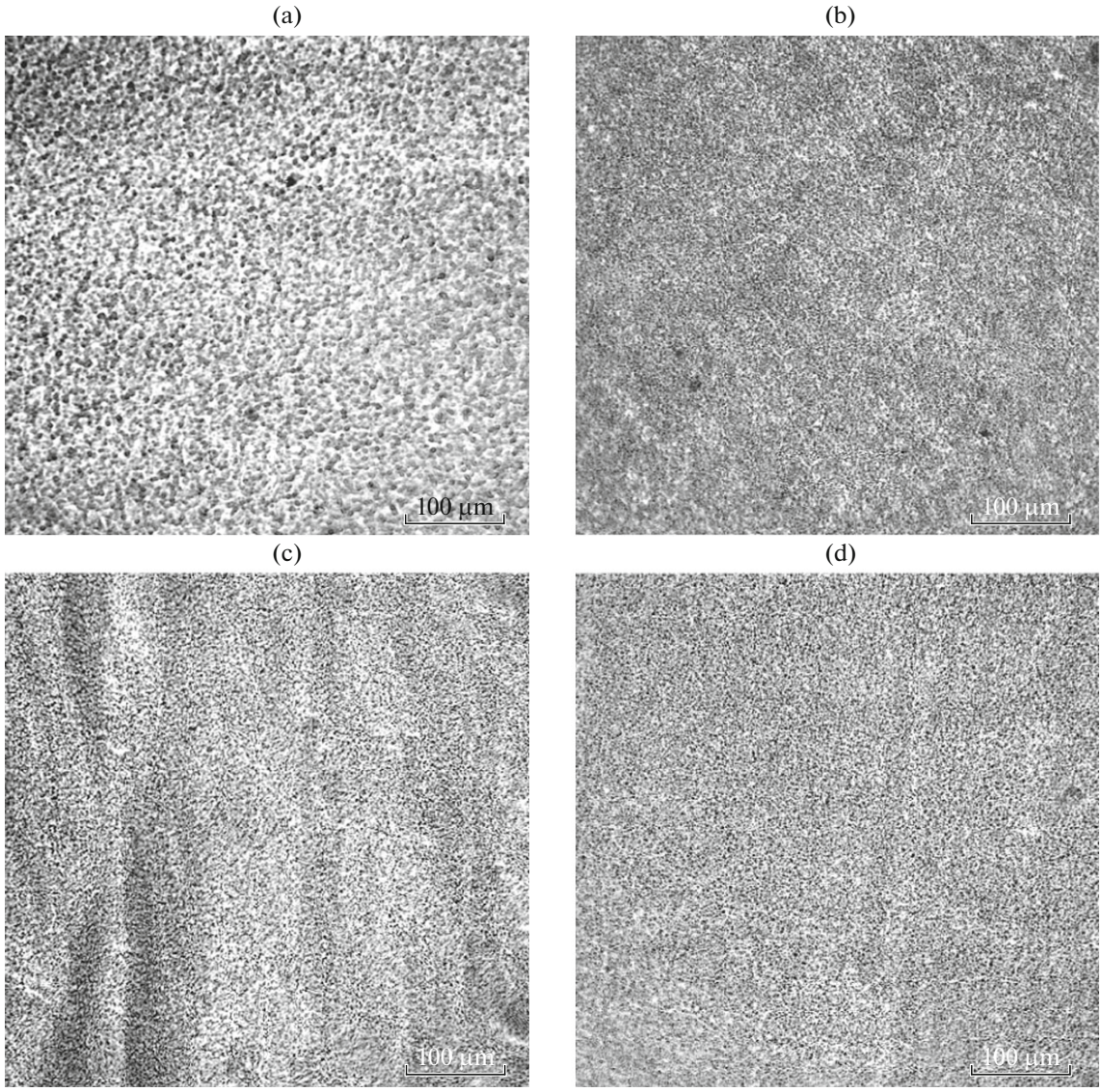

Fig. 2 Micrographs of composite PVACGs thin sections (a, b) perpendicular and (c, d) parallel to the axes of cylindrical samples formed from aqueous mixed solutions of PVA and ChHC with the subsequent transformation in ChHC into Ch. Initial concentrations of PVA and ChHC, respectively, are (a, c) 120 and 56 and (b, d) 120 and 112 g/L.

water–agarose systems [44–46]. However, in the case of the ChHC-free samples, no differences in the porous morphology of the lower and the upper surfaces of 1-mm discs could be seen at the used magnifications (Figs. 3a, 3b, 4a, 4b). Most likely, the ice crystallization front quickly overcame the thin layer of the polymer solution being frozen and the ice particles "had no time" to change their geometry, as they usually do in thicker layers because of unequal growth rates of different faces of such crystals [47].

When the initial solutions were frozen, the crystallization front moved upward; therefore, the micrographs in Figs. 3 and 4 are arranged in the same "order": the images of the lower surfaces of PVACG discs are, first, shown in the left-hand column, and, then, the micrographs of the upper layers of corresponding samples are shown in the right-hand column. After 1-mm discs of complex cryogels were formed, they were washed with water to remove soluble components (ChHC, NaCl, and the sol fractions of PVA that had not been embedded into the supramolecular network, because the yield of the cryotropic gelation of the polymer is not quantitative [47, 48]). Therefore, the micrographs in Figs. 3 and 4 show the macroporous morphology of the lower and upper regions of namely the PVA phase stained with Congo red (see Experimental).

The comparison between the samples formed from PVA solutions with and without salt in the absence of ChHC and the samples obtained from mixed solutions of the gelling and nongelling polymers showed a number of specific effects.

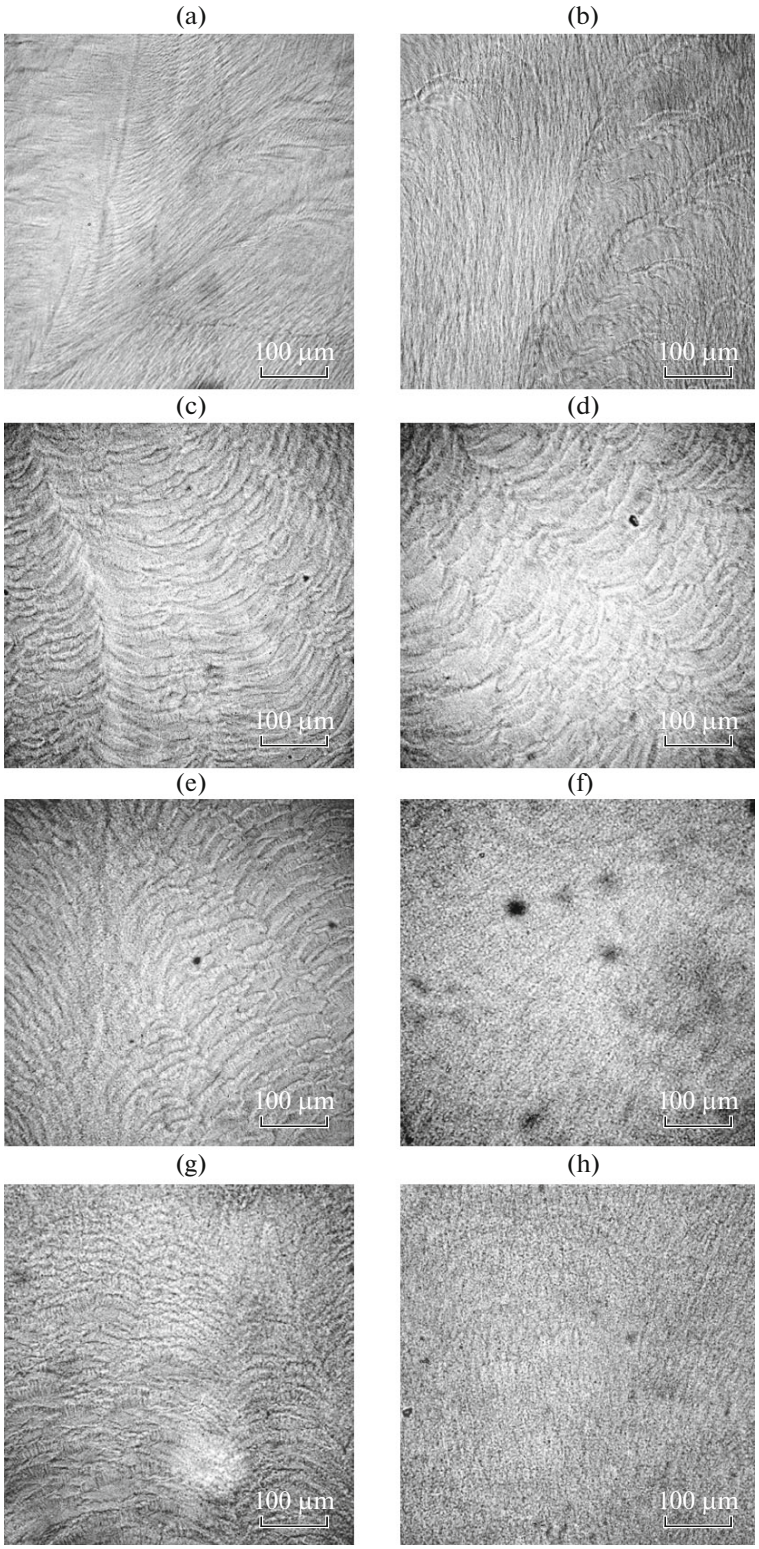

Fig. 3. Micrographs of the (a, c, e, g) lower and (b, d, f, h) upper surfaces of 1-mm discs of PVACGs and complex cryogels formed from aqueous mixed solutions of PVA and ChHC. Initial concentrations of PVA and ChHC, respectively, are (a, b) 120 and 0, (c, d) 120 and 56, (e, f) 120 and 112, and (g, h) 120 and 156 g/L.

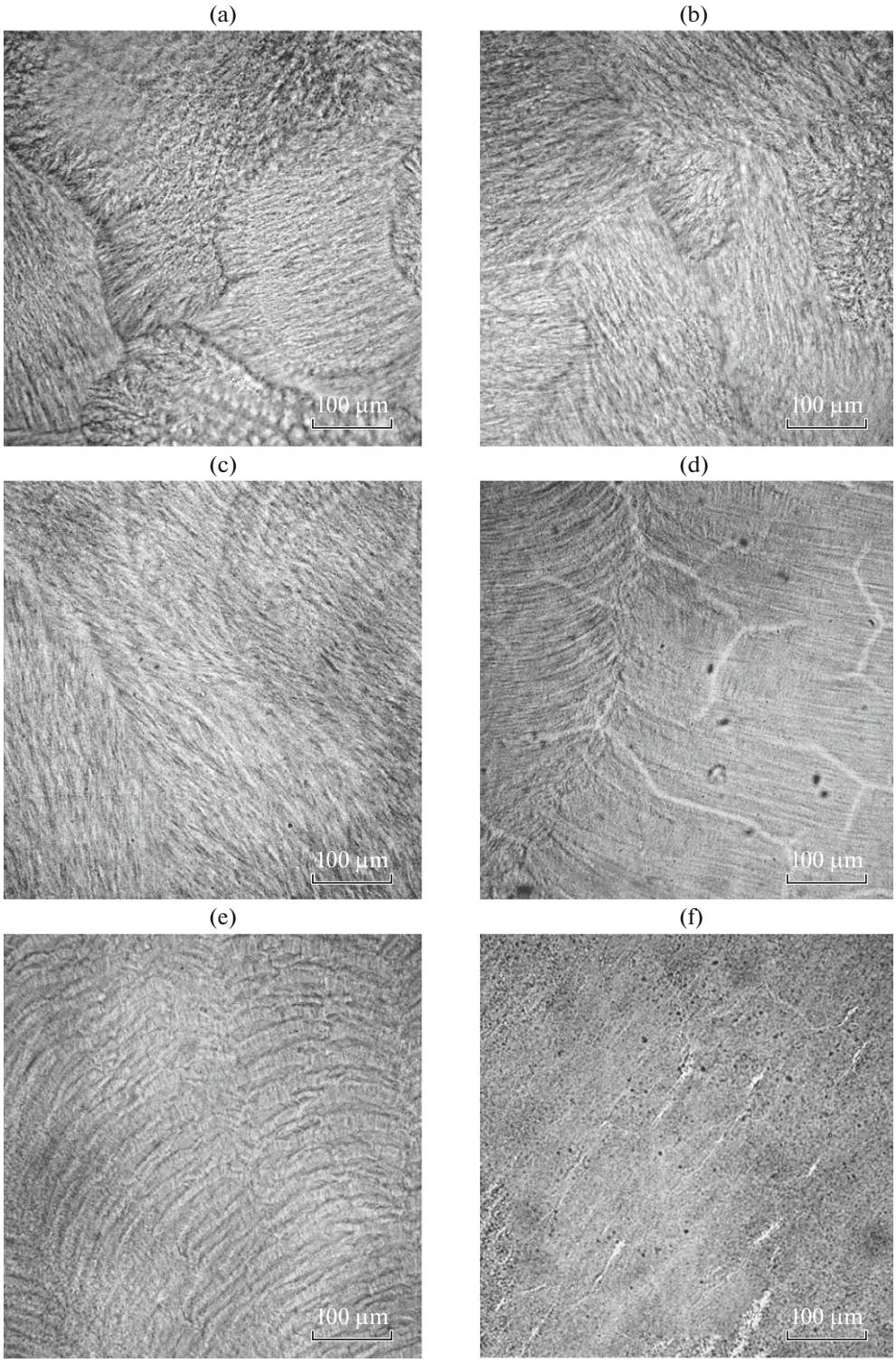

Fig. 4. Micrographs of the (a, c, e) lower and (b, d, f) upper surfaces of 1-mm discs of PVACG and complex cryogels formed from water–NaCl (0.15 M)–PVA–ChHC solutions. Initial concentrations of PVA and ChHC, respectively, are (a, b) 120 and 0, (c, d) 120 and 56, and (e, f) 120 and 112 g/L.

For example, in the case of PVACGs prepared from water–PVA–ChHC solutions, the most pronounced changes in the microstructure of the samples with an increase in the concentration of the nongelling polymer were observed for the upper surfaces of the gel discs (Figs. 3b–3h), while the general character of the morphology of their lower surfaces (Figs. 3c–3g) did not change significantly. Even when a small amount

(56 g/L) of ChHC was added to the initial system, cross-sectional sizes of the pores increased on both the lower and upper surfaces of formed PVACGs, as compared with the ChHC-free cryogel samples (compare Figs. 3a, 3b and 3c, 3d). However, the increase in the ChHC concentration to 112 g/L and, then, to 156 g/L led to a decrease in the pore sizes. These changes in the porous morphology were most pronounced for the upper surfaces of PVACG discs (Figs. 3f, 3h), i.e., in the course of freezing of a layer even as thin as 1 mm of a mixed PVA–ChHC solution, an obvious anisotropy appeared in the geometry of porogen particles, i.e., ice microcrystals. Moreover, the higher the ChHC concentration in a system being frozen, the more pronounced the anisotropy and the smaller the size of macropores at the upper surface of a cryogel disc. The observed character of the influence of ChHC on PVACG microstructure indicates a resistance created by the dissolved polymer salt to the growth of ice crystals, which is accompanied by the displacement of the unfrozen part of the liquid into the intercrystalline space and the region above the crystallization front.

As in the case of thin sections of the investigated PVACGs (Fig. 1), the microstructure of the preparations formed as 1-mm discs from water–NaCl–PVA and water–NaCl–PVA–ChHC precursor solutions (Fig. 4) was slightly different from the microstructure of the samples with the same concentrations of PVA and ChHC and free of the low-molecular-weight salt (Fig. 3). Primarily, it should be noted that we failed to obtain preparations of complex PVACG with a quality necessary for their microscopic examination from NaCl-containing solutions of the polymers with the highest ChHC concentration (156 g/L). After such cryogels were washed from the sol fraction, their shape could not be retained. Therefore, Figs. 4c–4f show the images of the lower and the upper surfaces of the discs obtained by cryogenic treatment of the solutions containing only 56 and 112 g/L ChHC. Similarly to the NaCl-free samples (Fig. 3), the changes in the macroporous morphology of PVACGs caused by the presence of ChHC in frozen solutions were more pronounced for the upper surfaces of the gel discs (Figs. 4d, 4f), as compared with the lower surfaces (Figs. 4c, 4e). As the initial ChHC concentration was increased, the cross-sectional sizes of macropores in the upper part of the discs markedly decreased (compare Figs. 4d and 4f), and even "discontinuities" (extended light formations resembling cracks) were observed in the structure. As was previously found [29], the used PVA and ChHC samples are compatible in a common solvent in a wide range of concentrations of both polymers. Meanwhile, at a certain concentration of the polymers, phase separation into two liquid phases may take place in the water–NaCl (0.15 M)–PVA–ChHC system, with one phase being enriched with gelling (upon the cryogenic treatment) PVA and the other phase being enriched with nongelling ChHC. Therefore, we assumed that the discussed peculiarities of the macroporous morphology of the cryogels (Figs. 4c–4f) might be due to the processes of liquid-phase separation in addition to the above-discussed influence of ChHC on the growth of porogen particles, i.e., ice crystals.

In this context, certain information on the component compositions of the lower and the upper parts of the discs formed from complex PVA cryogels was obtained by studying these objects with the help of ATR IR spectroscopy.

A Study of the Structure of Complex and Composite PVACGs by FTIR Spectroscopy

IR spectra of dry powdered polymer components of the studied complex and composite PVACGs, i.e., PVA, ChHC, and Ch, are shown in Fig. 5a. The spectra measured for these compounds have been described in detail elsewhere; in particular, for PVA [49, 51], ChHC [52, 53], and Ch [54, 55]. Since the cryogels contain a rather large amount of water, in order to make the subsequent interpretation of the spectral data more convenient, the most intense PVA and chitosan bands were chosen as analytical ones. For PVA, they were the band at 1420 cm^{-1} attributed to bending (wagging) vibrations of CH_2 groups, the band at 1328 cm^{-1} assigned to CH + OH bending vibrations with mixed frequency and shape, and the band at 1090 cm^{-1} inherent in the stretching vibrations of C–O bonds broadened toward lower frequencies. The band at 1142 cm^{-1}, which is also attributed to the C–O vibrations, is used to judge the degree of crystallinity of PVA. A low intensity of this band (Fig. 5a, spectrum *1*) attests to a low degree of crystallinity of initial dry PVA [49, 51]. ChHC was characterized by the bands assigned to the asymmetric and symmetric vibrations of NH_3^+ groups and the intense band with a maximum at 1063 cm^{-1}, which consists of a series of overlapping bands (1086, 1034, and 1015 cm^{-1}) attributed to the stretching vibrations of C–O–C and/or C–OH bonds. The band at 1154 cm^{-1} assigned to the C–O–C vibrations of glycoside bridges should be especially noted [52, 53]. The closeness of the bands at 1154 cm^{-1} in the ChHC spectrum and at 1142 cm^{-1} in the PVA spectrum greatly complicates the evaluation of the crystallinity of the latter in its composites with ChHC. In the spectrum of Ch, the absorption in the region of 1585 cm^{-1} is assigned to the bending vibrations of NH_2 groups, while the band at 1150 cm^{-1} is attributed to the stretching vibrations of C–O–C glycoside bridges. The maxima of absorption bands at 1065 and 1021 cm^{-1} correspond to the symmetric and asymmetric vibrations of C–O–C bands in pyranose rings, with their frequency being mixed with the stretching vibrations of C–OH groups [54, 55].

To clarify the effects relevant to the solvation of the polymers and its contribution to the spectral data on

the structure of the cryogels, the spectra were measured for PVA (120 g/L) and ChHC (112 g/L) solutions (Fig. 5b), as well as their mixed solution corresponding to the water content in complex PVACGs. Since the intensities of even the strongest bands in the initial spectra appeared to be rather low, Fig. 5b shows fragments of difference spectra obtained by subtracting the water spectrum. As might be expected, the transition from the solid state (powders) to the aqueous solutions was accompanied by two types of effects caused by solvation.

First, the majority of bands are narrowed and shifted. As a result, some of overlapping bands (e.g., the complex contour of enveloping bands in a range of 1200–900 cm^{-1}) in the ChHC spectrum (Fig. 5a, spectrum *2*) are resolved as separate peaks (Fig. 5b, spectrum *2*). Moreover, additional bands (or shoulders of bands) masked by overlapping of broadened bands characteristic of the solid state of the compounds have become clear. The above-described effects have been discussed in the literature [49, 53, 54], and they are clearly observed when the spectra in Figs. 5a and 5b are compared.

Second, the interaction of the polymers with water results in the formation of hydrogen bonds, which is reflected in shifts and changes in relative intensity and a shape of the contour of spectral bands attributed to the functional groups forming these bonds (Fig. 5b). It should, however, be noted that the mentioned changes in the spectra are relatively weak. It is, e.g., known that, upon the formation of H-bonds, the bands assigned to the bending vibrations of NH_2 and/or NH_3^+ groups are shifted to higher frequencies by, on average, 5–20 cm^{-1}; therewith, the bands attributed to asymmetric vibrations of N–H bonds exhibit a somewhat stronger response to the formation of H-bonds [54]. In our case, the high-frequency shift of the band assigned to asymmetric vibrations of NH_3^+ groups in the difference spectrum of an aqueous ChHC–PVA mixed solution (Fig. 5b, spectrum *3*) has resulted in almost complete disappearance of this band (the region of 1620 cm^{-1}). In the original spectrum (before water contribution was subtracted), the ν_{as} band for NH_3^+ groups appeared as a weak shoulder at 1590 cm^{-1} of the low-frequency wing of the broad band with a maximum at 1638 cm^{-1} attributed to the bending vibrations of water.

As might be expected, the effects found in the FTIR spectra of PVA and ChHC solutions (Fig. 5b) were also observed in the spectra of the cryogels. Figure 5c shows the spectra of 1-mm PVACG discs (*1*) free of the soluble chitosan salt, the (*2*) upper and (*3*) lower surfaces of the water–PVA–ChHC complex cryogel, and the (*4*) upper and (*5*) lower surfaces of the water–PVA–Ch composite cryogel obtained from the

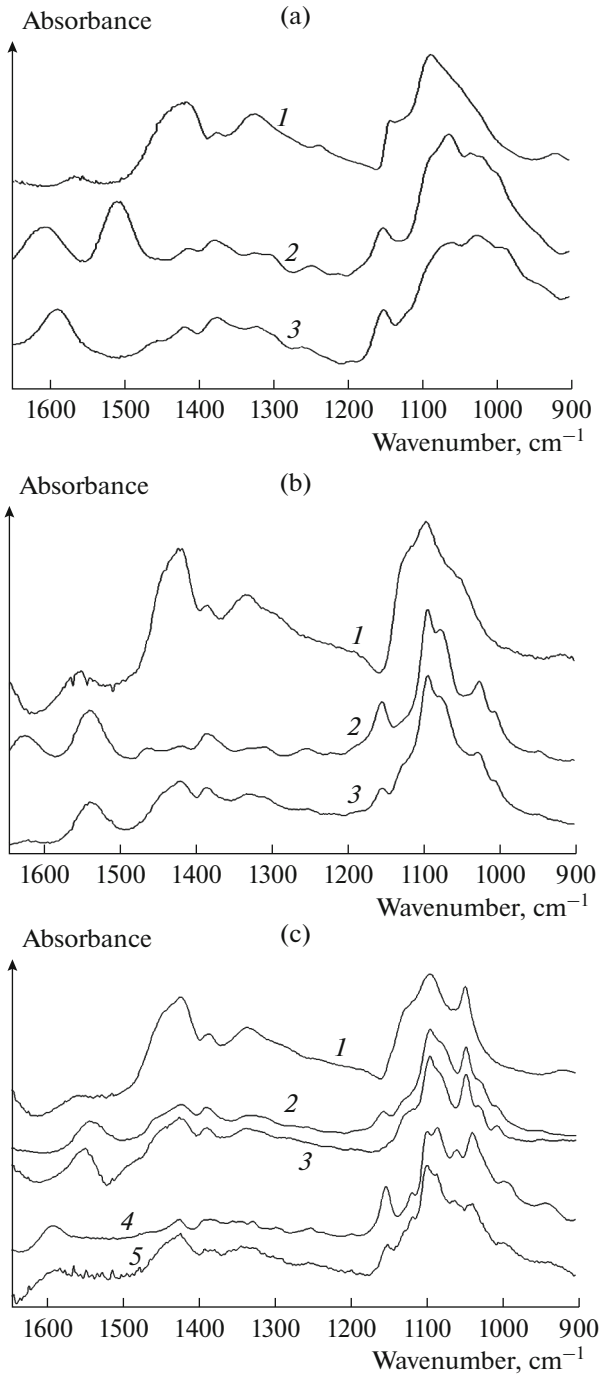

Fig. 5. FTIR spectra of the objects of the study: (a) spectra of dry powdered polymer components of complex and composite PVACGs: (*1*) PVA, (*2*) ChHC, and (*3*) Ch; (b) spectra of aqueous solutions (after subtracting contribution of water) of the polymer components of complex PVACGs: (*1*) PVA (120 g/L), (*2*) ChHC (112 g/L), and (*3*) PVA + ChHC (120 + 112 g/L); and (c) spectra of cryogels (after subtracting contribution of water): (*1*) cryogel of PVA (120 g/L) without additives, (*2*) the upper surface of a 1-mm disc of a complex cryogel containing PVA (120 g/L) and ChHC (112 g/L), (*3*) the lower surface of the disc of the same complex PVACG, (*4*) the upper surface of a water–PVA–Ch composite cryogel obtained by alkaline treatment of the complex PVACG with the composition similar to the sample for which spectra *2* and *3* were measured, and (*5*) the lower surface of the same composite PVACG.

complex cryogel by the alkaline treatment transformation of ChHC into Ch.

The spectra of these cryogels exhibited numerous effects, such as shifts of the bands and changes in the shape of their contour and their relative intensities. Some of these effects have been discussed above and are due to the formation of hydrogen bonds between the functional groups of the polymers and the solvent. The comprehensive analysis of the above-listed changes requires a separate specialized spectroscopic study. Nevertheless, the FTIR spectra shown in Fig. 5c lead us to make some conclusions, which are of importance for understanding the characteristics of the microstructure of the discussed PVACGs.

First, the spectra of the upper and the lower surfaces of complex PVACGs (Fig. 5c, spectra *2* and *3*, respectively) have appeared to be almost identical, with the exception of a small peak with a maximum at 1154 cm^{-1} attributed to the C–O–C vibrations of the glycoside bridges of pyranose rings of chitosan (to be more exact, its salt form). This peak is present in the spectrum of the upper cryogel surface and absent in the spectrum of the lower one.

On the contrary, in the case of the composite PVACG obtained by deprotonation of ChHC in the complex cryogel, the differences between the spectral characteristics of the upper and the lower surfaces of a disc 1 mm thick have appeared to be considerable. For example, the spectrum of the upper surface of the composite cryogel (Fig. 5c, spectrum *4*) exhibits a well-resolved broad band with a maximum at 1585 cm^{-1} attributed to the bending vibrations of NH_2 groups, as well as a group of bands in the region of 1200–900 cm^{-1} assigned to pyranose rings, while, in the spectrum of the lower surface of the sample (Fig. 5c, spectrum *5*), the aforementioned bands are very weak. At the same time, this IR spectrum contains bands at 1420, 1328, and 1090 cm^{-1}, which are mainly characteristic of PVA (compare with spectrum *1* in Fig. 5a). Thus, the data obtained indicate the existence of concentration gradients for the components in the water–PVA–Ch composite cryogel even at a preparation thickness as small as 1 mm; i.e., its lower and upper surfaces are enriched with PVA, and Ch, respectively.

This gives rise to a reasonable question: why are such gradients in the distributions of the gelling and nongelling polymers along the thickness of a 1-mm disc almost unobserved in the IR spectra of the complex PVACGs (Fig. 5c, spectra *2*, *3*)? In our opinion, this may be due to some technical features of the experiments. The fact is that composite cryogels were obtained immediately after the formation of discs of complex PVACGs by placing them in ammonia vapor [29]. Ammonia diffused into the cryogel matrix and deprotonated dissolved ChHC to transform it into Ch microparticles. After additional alkaline treatment and washing with water, such samples of composite cryogels were studied by FTIR spectroscopy. In turn, the discs of the complex water–PVA–ChHC cryogels were stored for some time before the spectroscopic examination; i.e., there were conditions for a gradual leveling of the concentration of soluble ChHC over the section of the preparation. Apparently, that is why significant differences could not be seen between the spectra of the upper and lower surfaces of the complex PVACGs (Fig. 5c, spectra *2*, *3*). Nevertheless, the optical microscopy (Figs. 3, 4) and IR spectroscopy (Fig. 5c) data on corresponding 1-mm discs of PVACGs indicate not only the difference between the sizes of macropores near their upper and lower surfaces, but also the existence of gradients in the distributions of PVA and ChHC over the thickness of the preparations, with the gradients being induced by phase separation during system freezing and displacement of more soluble components into the region before the ice crystallization front. Therefore, the upper part of a formed cryogel sample is enriched with ChHC (or Ch after alkaline treatment), while its lower part is characterized by a higher PVA concentration.

CONCLUSIONS

In work [29], which is devoted to the preparation and study of complex and composite PVACGs containing, respectively, water-soluble chitosan hydrochloride or water-insoluble microparticles of chitosan base incorporated into the continuous phase of macroporous PVACGs as a dispersion filler, we have shown that the rigidity and heat endurance of the obtained cryogels increase with the contents of the aforementioned forms of chitosan in them. It has been revealed that an important role in the integral properties of the cryogels is played by the structural factors, in particular, the macroporous morphology of the complex and composite PVACGs. Since various multicomponent complex and filled PVACGs draw increasing attention from the point of view of their practical use, especially as materials for biotechnological and biomedical applications [20–24, 55, 56], the study of factors significant for the physicochemical and service characteristics of such PVACGs is an urgent problem.

ACKNOWLEDGMENTS

This work was supported by the Program for Basic Research of the Division of Chemistry and Materials Sciences of the Russian Academy of Sciences "Development and Study of Macromolecules and Macromolecular Structures of New Generations" (p. 2: Nanostructures and Self-Organization in Functional Macromolecular Systems), Russian Foundation for Basic Research (project no. 15-04-07669), and the Ministry of Education and Science of the Russian Federation within the frameworks of the base part of a thematic plan.

REFERENCES

1. Nambu, M., *Kobunshi Ronbunshu*, 1990, vol. 47, p. 695.
2. Peppas, N.A. and Stauffer, S.R., *J. Control. Release*, 1991, vol. 16, p. 305.
3. Lozinskii, V.I., *Usp. Khim.*, 1998, vol. 67, p. 641.
4. Hassan, C.M. and Peppas, N.A., *Adv. Polym. Sci.*, 2000, vol. 153, p. 37.
5. Gutiérrez, M.C., Aranaz, I., Ferrer, M.L., and Del Monto, F., in *Macroporous Polymers: Production, Properties and Biological/Biomedical Applications*, Mattiasson, B., Kumar, A., and Galaev, I., Eds., Boca Raton: CRC, 2010, p. 83.
6. Gun'ko, V.M., Savina, I.N., and Mikhalovsky, S.V., *Adv. Colloid Interface Sci.*, 2013, vols. 187–188, p. 1.
7. Lozinsky, V.I., *Adv. Polym. Sci.*, 2014, vol. 263, p. 1.
8. Lazzeri, L., *Trends Polym. Sci.*, 1996, vol. 4, p. 249.
9. Surry, K.J.M., Austin, H.J.B., Fenster, A., and Peters, T.M., *Phys. Med. Biol.*, 2004, vol. 49, p. 5529.
10. Hoskins, P.R., *Ultrasound Med. Biol.*, 2008, vol. 34, p. 693.
11. Wan, W., Bannerman, A.D., Yang, L., and Mak, H., *Adv. Polym. Sci.*, 2014, vol. 263, p. 283.
12. Thomas, J., Gomes, K., Lowman, A., and Marcolongo, M., *J. Biomed. Mater. Res., Part B: Appl. Biomater.*, 2004, vol. 69, p. 135.
13. Pan, Y., Xiong, D., Chen, X., *J. Mater. Sci.*, 2007, vol. 42, p. 5129.
14. Sandeman, S.R., Gun'ko, V.M., Bakalinska, O.M., Howell, S.A., Zheng, Y., Kartel, M.T., Phillips, G.J., and Mikhalovsky, S.V., *J. Colloid Interface Sci*. 2011, vol. 358, p. 582.
15. Suzuki, A. and Sasaki, S., *J. Eng. Med.*, 2015, vol. 229, p. 828.
16. Lozinskii, V.I., Vakula, A.S., and Zubov, A.L., *Biotekhnologiya*, 1992, no. 4, p. 5.
17. Varfolomeev, S.D., Rainina, E.I., and Lozinsky, V.I., *Pure Appl. Chem.*, 1992, vol. 64, p. 1193.
18. Lozinsky, V.I. and Plieva, F.M., *Enzyme Microb. Technol.*, 1998, vol. 23, p. 227.
19. Lozinsky, V.I., Plieva, F.M., Galaev, I.Yu., and Mattiasson, B., *Bioseparation*, 2001, vol. 10, p. 163.
20. Lozinsky, V.I., Galaev, I.Yu., Plieva, F.M., Savina, I.N., Jungvid, H., and Mattiasson, B., *Trends Biotechnol.*, 2003, vol. 21, p. 445.
21. Plieva, F.M., Galaev, I.Y., Noppe, W., and Mattiasson, B., *Trends Microbiol.*, 2008, vol. 16, p. 543.
22. Lozinskii, V.I., *Izv. Ross. Akad. Nauk, Ser. Khim.*, 2008, p. 996.
23. Stolarzewicz, I., Bialecka-Florjańczyk, E., Majewska, T., and Krzyczkowska, J., *Chem. Biochem. Eng. Q.*, 2011, vol. 25, p. 135.
24. Mattiasson, B., *Adv. Polym. Sci.*, 2014, vol. 263, p. 245.
25. Altunina, L.K., Kuvshinov, V.A., and Dolgikh, S.N., *NATO Sci. Ser. IV, Earth Environ. Sci.*, 2006, vol. 65, p. 103.
26. Vasiliev, N.K., Ivanov, A.A., Sokurov, V.V., Shatalina, I.N., and Vasilyev, K.N., *Cold Reg. Sci. Technol.*, 2012, vol. 70, p. 94.
27. Vasiliev, N.K., Pronk, A.D.C., Shatalina, I.N., Janssen, F.H.M.E., and Houben, R.W.G., *Cold Reg. Sci. Technol.*, 2015, vol. 115, p. 56.
28. Altunina, L.K., Fufaeva, M.S., Filatov, D.A., Svarovskaya, L.I., Rozhdestvenskii, E.A., and Gan-Erdene, T., *Pochvovedenie*, 2014, p. 563.
29. Podorozhko, E.A., Ul'yabaeva, G.R., Kil'deeva, N.R., Tikhonov, V.E., Antonov, Yu.A., Zhuravleva, I.L., and Lozinsky, V.I., *Colloid J.*, 2016, vol. 78, p. 90.
30. Kulikov, S., Tikhonov, V., Blagodatskikh, I., Bezrodnykh, E., Lopatin, S., Khairullin, R., Philippova, Y., and Abramchuk, S., *Carbohydr. Res.*, 2012, vol. 87, p. 545.
31. Lozinsky, V.I., Damshkaln, L.G., Kurochkin, I.N., and Kurochkin, I.I., *Colloid J.*, 2007, vol. 69, p. 747.
32. Podorozhko, E.A., Lunev, I.A., Ryabev, A.N., Kil'deeva, N.R., and Lozinsky, V.I., *Colloid J.*, 2015, vol. 77, p. 186.
33. Lozinsky, V.I., Sakhno, N.G., Damshkaln, L.G., Bakeeva, I.V., Zubov, V.P., Kurochkin, I.N., and Kurochkin, I.I., *Colloid J.*, 2011, vol. 73, p. 234.
34. *Voda i vodnye rastvory pri temperaturakh nizhe 0°C* (Water and Aqueous Solutions at Temperatures Below 0°C), Franks, F., Ed., Kiev: Naukova Dumka, 1985.
35. Wang, S., Amornwittawat, N., Banatlao, J., Chung, M., Kao, Y., and Wen, X., *J. Phys. Chem. B*, 2009, vol. 113, p. 13891.
36. Okay, O., *Prog. Polym. Sci.*, 2000, vol. 25, p. 711.
37. Lozinsky, V.I. and Okay, O., *Adv. Polym. Sci.*, 2014, vol. 263, p. 49.
38. Okay, O. and Lozinsky, V.I., *Adv. Polym. Sci.*, 2014, vol. 263, p. 103.
39. Sergeev, G.B. and Batyuk, V.A., *Usp. Khim.*, 1976, vol. 45, p. 793.
40. Lozinsky, V.I., Solodova, E.E.V., Zubov, A.L., and Simenel, I.A., *J. Appl. Polym. Sci.*, 1995, vol. 58, p. 171.
41. Shapiro, Y.E. and Shapiro, T.I., *J. Colloid Interface Sci.,* 1999, vol. 217, p. 322.
42. Lozinsky, V.I., Damshkaln, L.G., Ezernitskaya, M.G., Glotova, Y.K., and Antonov, Y.A., *Soft Matter*, 2012, vol. 8, p. 8493.
43. Podorozhko, E.A., D'yakonova, E.A., and Lozinsky, V.I., *Colloid J.*, 2015, vol. 77, p. 46.
44. Yokoyama, F., Achife, E.C., Momoda, J., Shimamura, K., and Monobe, K., *Colloid Polym. Sci.*, 1990, vol. 268, p. 552.
45. Lozinsky, V.I., Damshkaln, L.G., Bloch, K.O., Vardi, P., Grinberg, N.V., Burova, T.V., and Grinberg, V.Ya., *J. Appl. Polym. Sci.*, 2008, vol. 108, p. 3046.
46. Plieva, F.M., Galaev, I.Yu., and Mattiasson, B., in *Macroporous Polymers: Production, Properties and Biological/Biomedical Applications*, Mattiasson, B.,

Kumar, A., and Galaev, I., Eds., Boca Raton: CRC, 2010, p. 131.

47. Lozinsky, V.I., Zubov, A.L., Savina, I.N., and Plieva, F.M., *J. Appl. Polym. Sci.*, 2000, vol. 77, p. 1822.
48. Kokabi, M., Sirousazar, M., and Hassan, Z.V., *Eur. Polym. J.*, 2007, vol. 43, p. 773.
49. Dechant, J., Danz, R., Kimmer, W., and Schmolke, R., *Ultrarotspektroskopische Untersuchungen an Polymeren*, Berlin: Akademie, 1972.
50. Krimm, S., Liang, C.Y., and Sutherland, G.B.B.M., *J. Polym. Sci.*, 1956, vol. 22, p. 227.
51. Pawlak, A. and Mucha, M., *Thermochim. Acta*, 2003, vol. 396, p. 153.
52. Brugnerotto, J., Lizardi, J., Goycoolea, F.M., Arguelles-Monal, W., Desbrieres, J., and Rinaudo, M., *Polymer*, 2001, vol. 42, p. 3569.
53. Bellamy, L.J., *The Infrared Spectra of Complex Molecules*, New York: Wiley, 1964, p. 2.
54. Smith, A., *Applied Infrared Spectroscopy*, New York: Wiley, 1979.
55. Wan, W., Bannerman, A.D., Yang, L., and Mak, H., *Adv. Polym. Sci.*, 2014, vol. 263, p. 283.
56. Kumar, A., *Supermacroporous Cryogels: Biomedical and Biotechnological Applications*, Boca Raton: CRC, 2016.

Translated by V. Kudrinskaya